Anal. Chem. **2007,** *79,* 6488−6495

Articles

Atomic Force Microscopy Investigation of the Morphology and the Biological Activity of Protein-Modified Surfaces for Bio- and Immunosensors

Francesca Cecchet,[†,#] Anne-Sophie Duwez,[*,†,‡] Sabine Gabriel,[§] Christine Jérôme,[§] Robert Jérôme,[§] Karine Glinel,[||] Sophie Demoustier-Champagne,[†] Alain M. Jonas,[†] and Bernard Nysten*[,†]

Unité de chimie et de physique des hauts polymères (POLY) and Research Center on Micro- and Nanoscopic Materials and Electronic Devices (CeRMiN), Université catholique de Louvain (UCL), Croix du Sud 1, B-1348 Louvain-la-Neuve, Belgium, Centre d'Etude et de Recherche sur les Macromolécules (CERM), University of Liège, B6a Sart-Tilman, B-4000 Liège, Belgium, and Polymères, Biopolymères, Membranes, UMR 6522−CNRS, University of Rouen, Bd Maurice de Broglie, F-76821 Mont Saint Aignan, France

With the purpose of developing biosensors, the reliable proof of the biological activity of two new sensor systems was obtained by atomic force microscopy (AFM) in both the imaging and the single-molecule force spectroscopy modes. Antigens or antibodies of pharmacological interest were grafted onto self-assembled monolayers of thiols on gold, and AFM imaging demonstrated that the grafting process produced homogeneous submonolayers of isolated proteins. The analysis of the morphology of the surfaces at the different functionalization steps allowed evaluating the protein grafting density and showed that the recognition of complementary species present in the surrounding solution occurred. Single-molecule force spectroscopy experiments between the sensing surfaces and AFM probes, onto which the complementary species were grafted, enabled a direct and rapid test of the biological activity of the sensors by investigating the interaction occurring at the level of one single ligand−receptor bond. Ellipsometry and surface plasmon resonance allowed further characterization of the sensor surfaces and confirmed that the biological recognition took place.

The proof of the biological activity of sensing surfaces is a major objective when developing the corresponding biodevice. Particularly, it is important to set up a general and versatile routine tool that is able to directly probe the biological activity of the sensing surface and that can be applied to any bio- or immunosensing surface, which is of interest for medicine or pharmacology. In this, atomic force microscopy (AFM) in the single-molecule force spectroscopy (SMFS) mode could be a rapid and reliable tool to provide information on the morphology as well as on the recognition abilities of such biological interfaces, down to the single-molecule level. Compared to surface plasmon resonance (SPR), a technique commonly used to investigate biological processes, single-molecule force spectroscopy holds several advantages. One main improvement is that, while SPR functions merely on metallic substrates, deposited as thin layers on glass, AFM measurements can be carried out on any substrate, that is, a metallic, or a semiconducting, or an insulating substrate, made of an organic or inorganic material, without restrictions of size or geometry. Moreover, while the detection ability of SPR is limited to few nanomolar of a 20-kDa protein, SMFS has no sensitivity limits as it is able to detect a single ligand−receptor bond, independent of the size of the species involved in the recognition process. In addition, SMFS requires only a little amount of complementary species to probe the biological activity of the sensor surface as only one or a few molecules onto the tips are needed to carry out reliable experiments. Another advantage is that SMFS is an almost noninvasive technique as it does not modify the sensor surface by adsorbing the complementary species (which may be difficult to remove) as it occurs in SPR experiments.

AFM has already proved its ability to characterize biologically modified surfaces as well as bio- or immunosensors. AFM imaging was used to image surfaces with grafted or adsorbed antigens (Ag) or antibodies (Ab) and to visualize the Ag/Ab recognition process for various systems such as bovine serum albumin (BSA) and anti-BSA IgG,[1] rabbit IgG Ab for immunoassays,[2] immun-

* Corresponding authors. E-mail: asduwez@ulg.ac.be; bernard.nysten@uclouvain.be.

[†] Université catholique de Louvain (UCL).

[#] Present address: Laboratory of Lasers and Spectroscopies, FUNDP−University of Namur, 61 rue de Bruxelles, B-5000 Namur, Belgium.

[‡] Present address: Université de Liège, Department of Chemistry B6a, Sart-Tilman, B-4000 Liège, Belgium.

[§] University of Liège.

[||] University of Rouen.

(1) Browning-Kelley, M. E.; Wadu-Mesthrige, K.; Hari, V.; Liu, G. Y. *Langmuir* **1997**, *13*, 343.

(2) Dong, Y.; Shannon, C. *Anal. Chem.* **2000**, *72*, 2371.

10.1021/ac070155q CCC: $37.00 © 2007 American Chemical Society
Published on Web 08/04/2007

Scheme 1. Schematic Representation of (a) the Covalent Grafting of Proteins onto the Surface of the Biological Device and of (b) a Biological Recognition Event Investigated by Single-Molecule Force Spectroscopy Experiment

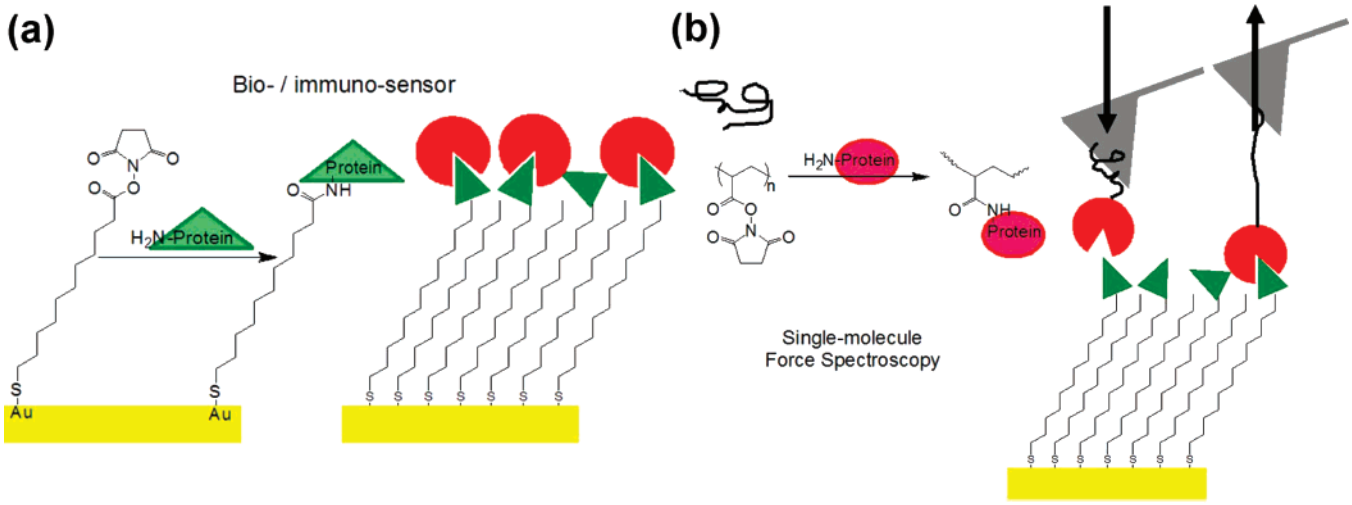

osensors for Salmonella,[3] or biosensors for pesticides.[4] Force spectroscopy is also known to be a remarkable tool for molecular recognition,[5] allowing the exploration of the biological activity of sensing surfaces. It was used by several authors to assess the biological activity and selectivity of bio- or immunosensor surfaces[4,6] or to analyze the influence of epitope availability on Ag/Ab interaction,[7] the Ab orientation on charged surfaces,[8] and the influence of surfactants on Ab orientation and hence on interaction specificity.[9] AFM-based molecular recognition is strongly dependent on the design of an accurate modification of the tips. One or few polymeric linkers need to be tightly tethered to the tip apex. Most of the procedures proposed so far to anchor molecules of interest onto SPM probes consist of multistep procedures, each specific application requiring its own chemical design. When no linker is used, sawtooth-like force curves resulting from multiple binding interactions are observed.[4] In such a case, it is always difficult to distinguish between specific ligand−receptor interactions and nonspecific adhesion.

Here we show that AFM, with basic commercial equipment, can be used as a "routine" technique to probe the biological activity of sensor surfaces of pharmacological interest (Scheme 1a), by detecting single ligand−receptor bonds (Scheme 1b), using a generic versatile linker. We have investigated the morphology and the biological activity of two new bio- or immunosensor devices. The sensor surfaces were built up by the well-known method of grafting proteins to *N*-succinimydil activated, acid-terminated, self-assembled monolayers of thiols on gold[10−21] (Scheme 1a). One system consists of the P.69 pertactin protein (also known as antigen 69K) grafted onto a surface recognizing its complementary antibody, anti-69K. Antigen 69K is a compact globular protein located in the outer membrane of *Bordetella pertussis* and is a key component of acellular vaccines against whooping cough.[22−24] The second system is based on the surface-grafted antibody 286F7, which is directed toward the thyroid stimulating hormone (TSH, also known as thyrotropin). TSH is produced by and stored in the pituitary gland, which is located beneath the brain, and its detection is used for the diagnosis of problems affecting the thyroid gland.

EXPERIMENTAL SECTION

Materials. 11-Mercaptoundecanoic acid (11-MUA, 95%) was purchased from Sigma-Aldrich. *N*-Hydroxysuccinimide (NHS, 98+%), 1-(3-dimethylaminopropyl)-3-ethylcarbodiimide hydrochloride (EDC, 98+%), potassium phosphate monobasic (KH_2PO_4, 99+%), and potassium phosphate dibasic (K_2HPO_4, 98%) were

(3) Oh, B. K.; Kim, Y. K.; Park, K. W.; Lee, W. H.; Choi, J. W. *Biosens. Bioelectron.* **2004**, *19*, 1497.
(4) Kaur, J.; Singh, K. V.; Schmid, A. H.; Varschney, G. C.; Suri, C. R.; Raje, M. *Biosens. Bioelectron.* **2004**, *20*, 284.
(5) Kienberger, F.; Andreas Ebner, A.; Gruber, H. J.; Hinterdorfer, P. *Acc. Chem. Res.* **2006**, *39*, 29.
(6) Allen, S.; Chen, X.; Davies, J.; Davies, M. C.; Dawkes, A. C.; Edwards, J. C.; Roberts, C. J.; Sefton, J.; Tendler, S. J. B.; Williams, P. M. *Biochemistry* **1997**, *36*, 7457.
(7) Allen, S.; Davies, J.; Davies, M. C.; Dawkes, A. C.; Roberts, C. J.; Tendler, S. J. B.; Williams, P. M. *Biochem. J.* **1999**, *341*, 173.
(8) Chen, S.; Liu, L.; Zhou, J.; Jiang, S. *Langmuir* **2003**, *19*, 2859.
(9) Brogan, K. L.; Shin, J. H.; Schoenfisch, M. H. *Langmuir* **2004**, *20*, 9729.
(10) Ferretti, S.; Paynter, S.; Russell, D. A.; Sapsford, K. E.; Richardson, D. J. *Trends Anal. Chem.* **2000**, *9*, 19.
(11) Allara, D. *Biosen. Bioelectron.* **1995**, *10*, 771.
(12) Higashi, N.; Takahashi, M.; Niwa, M. *Langmuir* **1999**, *15*, 111.
(13) Madoz, J.; Kuznztzov, B. A.; Medrano, F. J.; Garcia, J. L.; Fernandez, V. M. *J. Am. Chem. Soc.* **1997**, *119*, 1043.
(14) Blonder, R.; Willner, I.; Buckmann, F. *J. Am. Chem. Soc.* **1998**, *120*, 9335.
(15) Jordan, C. E.; Frey, B. L.; Kornguth, S.; Corn, R. M. *Langmuir* **1994**, *10*, 3642.
(16) Ostuni, E.; Yan, L.; Whitesides, G. M. *Colloids Surf. B: Biointerfaces* **1999**, *15*, 3.
(17) Gooding, J. J.; Hibbert, D. B. *Trends Anal. Chem.* **1999**, *8*, 18.
(18) Patel, N.; Davies, M. C.; Hartshorne, M.; Heaton, R. J.; Roberts, C. J.; Tendler, S. J. B.; Williams, P. M. *Langmuir* **1997**, *13*, 6485.
(19) Jiang, L.; Glidle, A.; Griffith, A.; McNeil, C. J.; Cooper, J. M. *Bioelectrochem. Bioenergetics* **1997**, *42*, 15.
(20) Yang, H. C.; Dermody, D. L.; Xu, C.; Ricco, A. J.; Crooks, R. M. *Langmuir* **1996**, *12*, 726.
(21) Strither, T.; Cai, W.; Zhao, X.; Hamers, R. J.; Smith, L. M. *J. Am. Chem. Soc.* **2000**, *122*, 1205.
(22) Podda, A.; Nencioni, L.; Marsili, I.; Peppoloni, S.; Volpini, G.; Donati, D.; Di Tommaso, A.; De Magistris, M. T.; Rappuoli, R. *Vaccine* **1991**, *9*, 741.
(23) Van Damme, P.; Burgess, M. *Vaccine* **2004**, *22*, 305.
(24) Gustafsson, L.; Hallander, H. O.; Reizenstein, E.; Storsaeter, J. *N. Engl. J. Med.* **1996**, *334*, 349.

supplied by Acros. Buffer phosphate was homemade (PBS; 20 mM K_2HPO_4 and KH_2PO_4, 0.15 M NaCl, pH 7.5). P.69 pertactin (69K Ag), having an ellipsoidal structure, with typical axis lengths of 10.6, 3.8, and 2.5 nm,[25,26] and its complementary monoclonal antibody (anti-69K Ab) were provided by GlaxoSmithKline Biologicals (Rixensart, Belgium). Anti-TSH monoclonal antibody (286F7 Ab, sizing 15 nm[2]) was provided by BiocodeHycel, and its complementary human TSH was purchased from NIBSC . The substrates were template-stripped gold (TSG) surfaces prepared as described elsewhere.[27,28]

Surface Biofunctionalization. 69K Ag or 286F7 Ab were covalently bonded to the gold surfaces following the widely used procedure,[10] which consists of functionalizing acid-terminated, self-assembled monolayer of 11-MUA bonded to gold. Carboxylic acid-terminated monolayers were prepared by immersion of the gold substrates in a 2 mM ethanol solution of 11-MUA for 17 h. The samples were rinsed in ethanol and dried under argon before functionalization. The carboxylic acid groups of the SAMs were activated by immersion in an aqueous solution of NHS (0.05 M) and EDC (0.2 M) for 30 min, followed by rinsing in water. The activated surfaces were then immersed in a solution of the antigen (69K Ag, 211 μg/mL in PBS) or of the antibody solution (286F7 Ab, 1.10 mg/mL in PBS) for 1 h and then abundantly rinsed with PBS and water. In order to deactivate residual NHS ester groups, the surfaces were immersed in an ethanolamine solution (0.1 M, pH 7.5 in PBS) for 30 min. The antibody−antigen interactions were performed by immersing the biofunctionalized gold surfaces in either anti-69K (1950 μg of IgG/mL in PBS) or TSH (2 μg/mL in PBS) solutions. After 1 h of association, the samples were copiously rinsed with PBS and water.

Ellipsometry. The thickness of the organic films was measured in air with a Jobin-Yvon Digisel single-wavelength (632.8 nm) rotating compensator ellipsometer. For these experiments, TSG surfaces were first prepared as described elsewhere.[27,28] The refractive index of these substrates was determined by fitting in the (Ψ,Δ) plane the ellipsometric trajectory corresponding to a set of samples consisting of PMMA layers of increasing thickness spin-coated onto TSG. The refractive index of our TSG substrates was thereby found to be 0.168−j3.668. The thickness of the thiol and protein layers was subsequently obtained by using this refractive index, assuming that the organic layers have a refractive index of 1.5. Although the real value of the refractive index of the layers may be anywhere between 1.4 and 1.6, our arbitrary selection is sufficient for our purposes, since varying the refractive index from 1.4 to 1.6 only resulted in variations of thickness of ~25%.

Surface Plasmon Resonance. SPR measurements were achieved by using a Multiskop SPR spectrometer (Optrel GbR) equipped with a He−Ne laser light (λ = 632.8 nm). The laser and detector arms were rotated synchronously using a two-arm goniometer with an angular resolution of 0.001°. A rotating Glan-Thompson polarizer (Halle) with an extinction ratio of 10^{-8} was used to control the p-polarization state of the incident laser light. The reflected light from the sample into a photodiode detector was recorded as a function of the angle of incidence. The SPR chip was assembled as Kretschmann ATR configuration with a 90° angle LASF9 prism using refractive index matching oil (diiodomethane and sulfur, Cargille). Moreover, the SPR chip, consisting of an LASF9 glass slide of which one face was coated by a thin layer of gold, was mounted onto a flow cell with a 4-mL volume. The buffer solution was introduced to the gold surface by syringe injection. All measurements were performed at 20 °C. Experimental data were fitted to theoretical reflectivity curves calculated from Fresnel equations using Spall software (Optrel GbR). A two-layer (layers 1 and 2) model was used to analyze the data with layer 1 and layer 2 designed as gold layer and protein layer, respectively. The refractive indices of the LASF9 substrate and buffer solution were taken to be 1.84 and 1.33, respectively. In a typical SPR experiment, a SPR chip was first tested in PBS buffer to determine the parameters of the gold layer. According to this measurement, the thickness and the refractive index of the gold layer were determined to be 46 nm and −0.216 (n) and 1.500 (k), respectively.

AFM Microscopy. AFM images were recorded in PBS solution in intermittent-contact mode (IC-AFM or tapping mode) with a PicoSPM equipped with a fluid cell (Molecular Imaging, Phoenix, AZ) and controlled by a Nanoscope IIIa electronics (Digital Instruments, Santa Barbara, CA). The cantilevers (Point-probe Force Modulation cantilevers from Nanosensors) were silicon cantilever beams of resonance frequency ~25 kHz in liquid and nominal spring constant of 2.8 N/m, with an integrated silicon tip with an apex radius of ≤10 nm. Soft-tapping conditions were used; i.e., the ratio between the set-point amplitude and the free amplitude of the cantilever vibration was always kept above 0.8.

Statistical analysis of the AFM images (roughness, particle size, and distribution) was realized using homemade procedures developed under Igor Pro (Wavemetrics, Inc.). The radial autocorrelation function of the images was computed as follows. The 2D autocorrelation function, 2DCF, was first computed as the inverse Fourier transform of the image power spectral density, i.e., the squared magnitude of the image Fourier transform.[29] The 2D autocorrelation function was then circular averaged to obtain the radial autocorrelation function (CF). This function is proportional to the probability that two points at a distance r have the same height. Thus, if the surface consists of uniformly and isotropically distributed objects of approximately the same size, the radial autocorrelation function should present maximums at distances corresponding to the average repeat distance of the objects, L_p. Information on the object average size and interdistance was obtained by computing the interface distribution function (IDF) of the images. In our case, we computed the IDF as the circular average of the chord distribution function, CDF, defined as the Laplacian of the 2DCF.[30] The position of two first maximums of the IDF corresponds to the average object size and interdistance, and the position of the first minimum corresponds to the object repeat distance.

Single-Molecule Force Spectroscopy. We used standard V-shaped silicon nitride cantilevers with pyramidal tips from Veeco

(25) Emsley, P.; Charles, I. G.; Fairweather, N. F.; Isaacs, N. W. *Nature* **1996**, *381*, 90.
(26) Pallandre, A.; De Meersman, B.; Blondeau, F.; Nysten, B.; Jonas, A. M. *J. Am. Chem. Soc.* **2005**, *127*, 4320.
(27) Wagner, P.; Hegner, M.; Güntherodt, H.-J.; Semenza, G. *Langmuir* **1995**, *11*, 3867.
(28) Baralia, G.; Duwez, A.-S.; Nysten, B.; Jonas, A. M. *Langmuir* **2005**, *21*, 6825.
(29) Pratt, W. K. *Digital Image Processing*, 2nd ed.; Wiley: New York, 1991.
(30) Haubruge, H. G.; Jonas, A. M.; Legras, R. *Macromolecules* **2004**, *37*, 126.

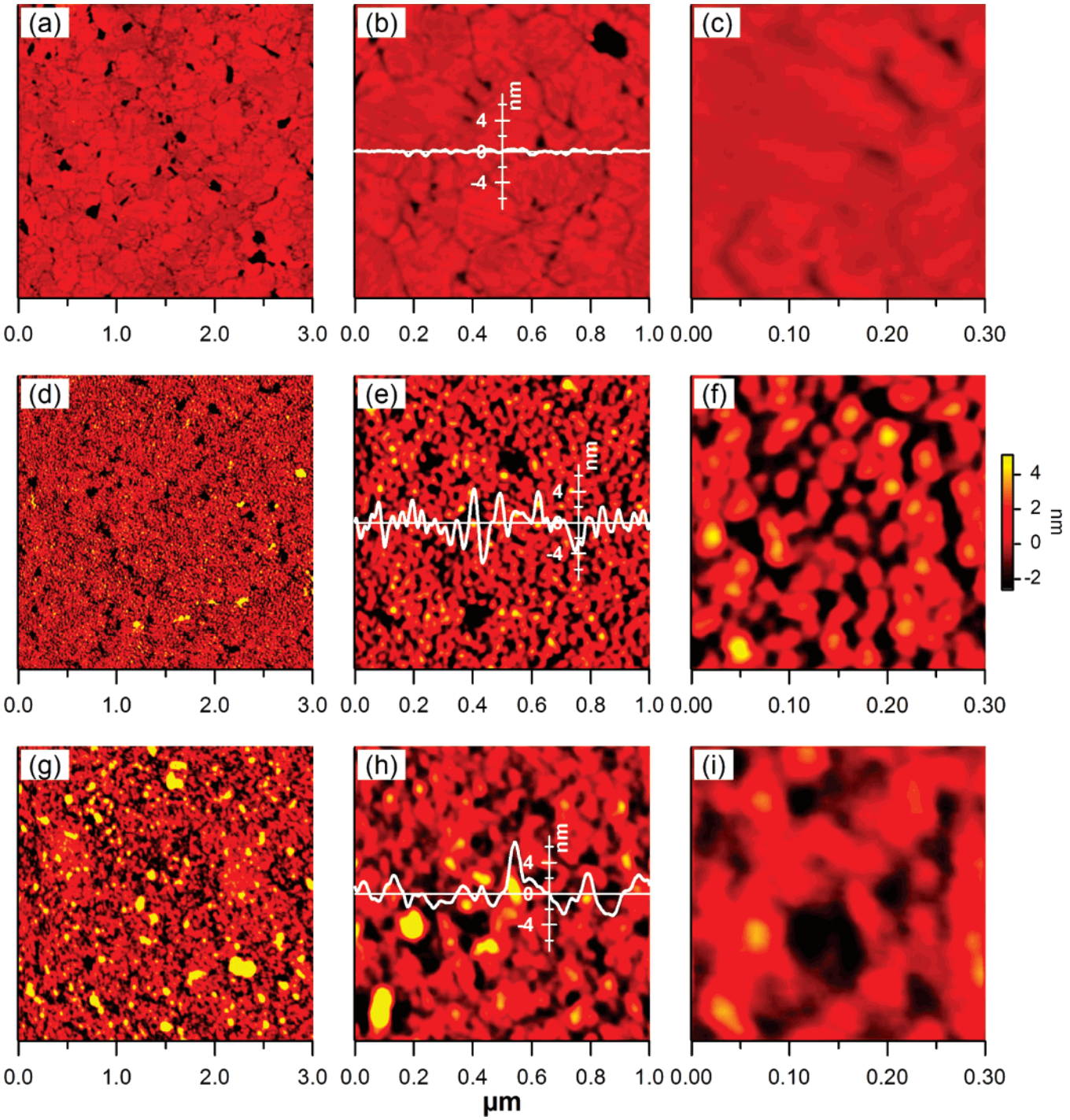

Figure 1. AFM height images for (a−c) a gold substrate, (d−f) 69K Ag grafted on 11-MUA SAM, and (g−i) 69K Ag/anti-69K Ab on 11-MUA SAM. Section profiles corresponding to the horizontal lines are superposed on the 1 × 1 μm^2 images (b, e, h).

Instruments (Microlevers). Proteins were covalently coupled to the tips by a two-step procedure. First, poly(*N*-succinimidyl acrylate) (PNSA) was grafted from the probes, using an electro-initiated process described elsewhere.[31] We chose electrografting conditions for which chains are grafted in an isolated chain regime; i.e., only one linker is grafted at the tip apex.[32] Hence, PNSA-modified tips were immersed in the opportune protein solution for 1 h and then in a PBS solution overnight. The proteins grafted onto the tips were anti-69K antibodies and TSH hormones, respectively. The spring constants of the cantilevers used were calibrated following the procedure reported in reference.[33] Approach−retraction curve measurements were performed at a loading rate of 96 nN/s for the 69K Ag/anti-69K Ab system and of 100 nN/s

(31) Jérôme, C.; Willet, N.; Jérôme, R.; Duwez, A.-S. *ChemPhysChem* **2004**, *5*, 147.

(32) Gabriel, S.; Jérôme, C.; Jérôme, R.; Fustin, C.-A.; Pallandre, A.; Plain, J.; Jonas, A. M.; Duwez, A.-S. *J. Am. Chem. Soc.* DOI: 10.1021/ja071723m.

(33) Dupres, V.; Menozzi, F. D.; Locht, C.; Clare, B. H.; Abbott, N. L.; Cuenot, S.; Bompard, C.; Raze, D.; Dufrêne, Y. F. *Nat. Methods* **2005**, *2*, 515.

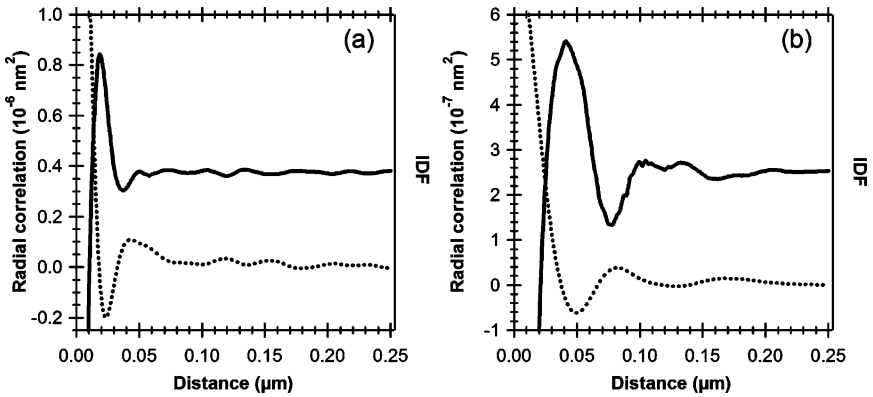

Figure 2. Radial autocorrelation function (dotted curves) and interface distribution function (solid curves) corresponding to a surface grafted with the 69K Ag (a) and to the same surface after contact with a solution containing the anti-69K Ab (b).

for the 286F7Ab/TSH system (Loading rate-dependent measurements are given in the Supporting Information). The deflection versus vertical displacement data were processed using a program developed under Igor Pro (WaveMetrics, Inc.) to convert curves into force versus distance curves and to extract from every curve the pull-off force. For each system, from the force-distance curves, a probability density function (pdfs) of forces was constructed resulting in a Gaussian distribution centered on the most probable unbinding force.

Table 1. Results of the Statistical Analysis of the AFM Images: σ, the rms Roughness, d, the Average Object Size, L_p, the Average Object Repeat Period, and the Surface Coverage[a]

system	σ (nm)	d (nm)	L_p (nm)	surface coverage (cm^{-2})
TSG	0.32 (0.09)			
Ag 69K	1.81 (0.40)	18.2 (1.5)	39.4 (6.6)	8.2×10^{10}
Ab−Ag 69K	1.47 (0.28)	35.8 (11.6)	94.4 (39.6)	1.4×10^{10}
Ab 286F7	0.52 (0.06)	20.4 (2.8)	57.3 (17.4)	3.9×10^{10}

[a] Standard deviations are given in parentheses.

RESULTS AND DISCUSSION

Surface Morphology. The morphology of the functionalized surfaces was investigated by ellipsometry and AFM. Ellipsometry provided thicknesses of 1.5, 2.1, and 3.6 nm for the thiol monolayer, the thiol monolayer after activation, and the film after grafting of the 69K protein, respectively. This corresponds to a value of 3.6−1.5 = 2.1 nm for the thickness of the Ag layer, a value smaller than the smallest dimension of the ellipsoidal protein, i.e., 2.5 nm. Since ellipsometry essentially provides the equivalent thickness of a fully dense organic layer, the thickness value suggests that 69K molecules are adsorbed or grafted in an incompletely filled layer, probably with the long axis of the proteins oriented parallel to the surface.

Figure 1 shows the topographical characteristics of the surfaces at different steps of the grafting procedure for the 69K system. The radial correlation functions and the interface distribution functions corresponding to images taken on surfaces after grafting of the 69K Ag and after dipping of these surfaces in a anti-69K Ab solution, respectively, are shown in Figure 2.

The unmodified gold substrate (Figure 1a−c), the 11-MUA SAM and the 11-MUA SAM activated by EDC−NHS (data not shown) all exhibit the same topographical features, where only flat gold terraces and grain boundaries are observed and with a rms roughness equal to 0.32 nm (Table 1).

The topographical images recorded after functionalization with the 69K Ag (Figure 1d−f) show new features and a rms roughness of ~1.8 nm, testifying to the presence of antigen molecules on the surface. The height, between 2 and 4 nm, of the objects (see section profiles in Figure 1e), is consistent with the diameter of the proteins. The average diameter of the objects obtained from the IDF (Figure 2a) is equal to 18.2 nm (Table 1) and is also consistent with the 69K Ag dimensions, taking into account the image dilation due to the tip size. The average protein repeat distance is equal to 39.4 nm. From this value, it is possible to evaluate a protein surface coverage, assuming that each protein occupies a surface of diameter equal to L_p. The as-evaluated surface coverage is equal to 8.2×10^{10} proteins/cm^2. If the cylindrical proteins were lying parallel to the surface and were completely covering the substrate, the surface coverage would be equal to 3.1×10^{12} cm^{-2}.

Combining the ellipsometry and the AFM results indicates that the proteins are adsorbed or grafted as isolated molecules in a homogeneous, but not fully dense, submonolayer. They are preferentially oriented with their long axis parallel to the surface. The adsorption geometry of proteins onto surfaces is usually due to several factors, i.e., the position of the binding site within the protein structure, the interactions between the whole protein with the underlying surface (hydrophobic interactions, hydrogen bonding, electrostatic interactions) and the environmental conditions (pH, ionic strength): we can resume by rationalizing that the adsorption geometry depends on the physical−chemical interactions occurring between the protein and the surface at the solid/liquid interface. In the framework of the development of a sensor surface, the adsorption geometry is in charge of the availability of the recognition sites of the proteins by their complementary species in the surrounding solution. When the protein structure or the adsorption geometry are unknown the availability of the active sites cannot be predicted but only probed a posteriori by detecting the recognition process in which they are involved.

After the dipping process in the anti-69K Ab solution, the topography of the surface showed new features indicating that anti-69K Ab proteins have adsorbed from the solution. The AFM images (Figure 1g−i) have a smaller roughness than the surfaces grafted with the Ag but they show the presence of larger objects.

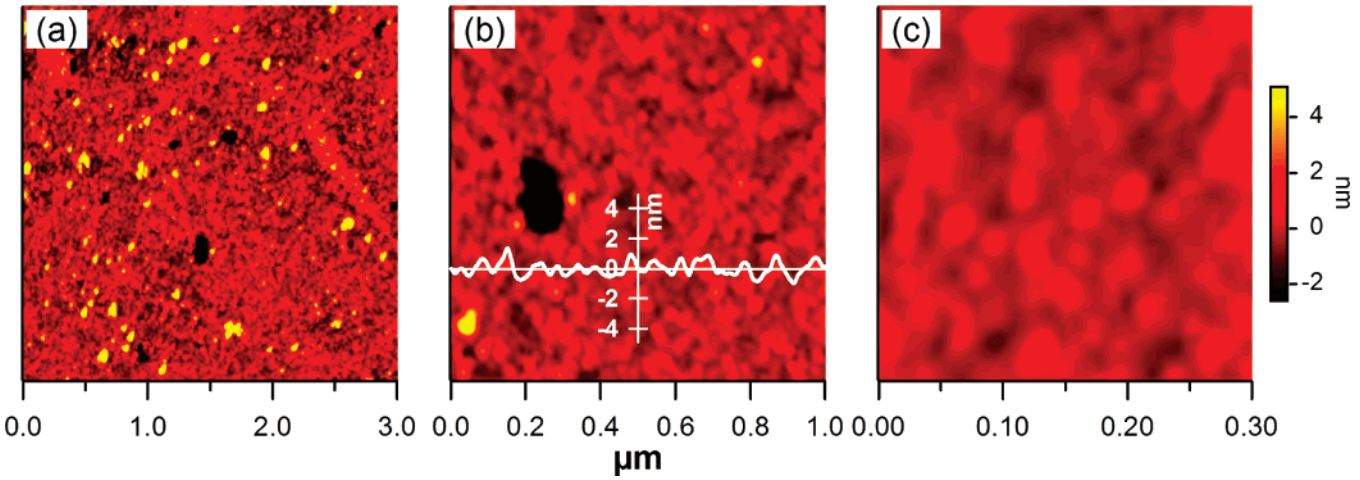

Figure 3. AFM height images for 286F7 Ab grafted on 11-MUA SAM. Section profile corresponding to the horizontal line is superposed to the $1 \times 1\ \mu m^2$ image.

The average size of these objects is equal to 35.8 nm. This value is larger than that measured on the surfaces grafted with the 69K Ag (18.2 nm) and also larger than that measured on surfaces with grafted anti-69K Ab (30.9 nm). This suggests that the objects observed on the AFM images correspond to the Ab−Ag complexes. The average repeat distance increases up to 94.4 nm, corresponding to a surface coverage of 1.4×10^{10} cm^{-2}. This lower surface coverage suggests that only a partial recognition of the antigens by the antibodies was achieved, possibly due to multiple mutual orientations of Ag and Ab at the interface or to a partial denaturation of the surface-confined antigen moieties. A rough evaluation gives approximately one recognition event for six antigens.

The thickness of the layer, as obtained by ellipsometry, increased up to 7.0 nm, which corroborates the complexation of antibodies on the antigen sensor surface.

The topographical characterization of the 286F7 Ab surface (Figure 3) provides similar information. The average size of the observed objects estimated from the autocorrelation function and the IDF is equal to 20.4 nm (Table 1) and is also compatible with the Ab dimensions. The surface coverage estimated from the average repeat distance, 57.3 nm, is equal to 3.9×10^{10} cm^{-2}, a value smaller than in the case of the 69K Ag. The functionalized surfaces thus consist of submonolayers of proteins, as demonstrated by the fact that gold boundaries between neighboring terraces are still observed (Figure 3a). Moreover, the protein distribution onto the surface is rather homogeneous, demonstrating again that the sensor surface is a uniform layer of mainly isolated molecules.

Surface plasmon resonance was used as reference standard technique to validate in situ that recognition occurred. Figure 4 shows the reflectivity curves versus the angle of incidence recorded in PBS buffer for a bare gold, 69K Ag film before and after recognition by anti-69K Ab. The reflection angle minimums progressively shift to higher values when going from the bare gold to the sensor surfaces and to the sensor surface after recognition by the complementary species. This behavior reflects the increased mass of the layer following the grafting of the sensor proteins onto the surfaces and next the formation of the Ag−Ab complexes, respectively. The thickness of the biological layers

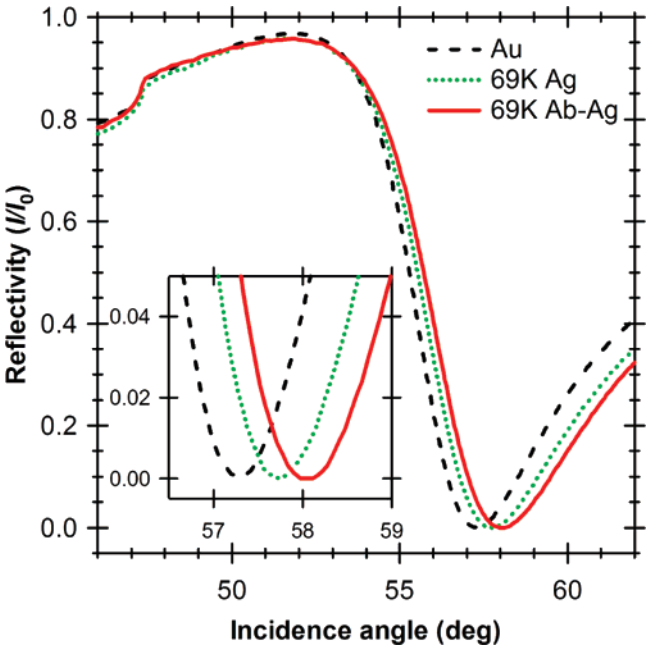

Figure 4. Reflectivity vs angle of incidence SPR curves recorded for a bare gold (black dashed curve), a 69K Ag film (green dotted curve) and for a 69K Ag film after recognition by anti-69K Ab (red solid curve), all taken in solution.

was obtained by fitting the raw data. The 69K Ag sensor surface was 4.0 nm thick, while after recognition by anti-69K Ab the thickness increased to 6.5 nm, in very close agreement with the data obtained by ellipsometry. While these results lack quantitative information on the yield of the recognition process, they validate that recognition occurred at the solid/liquid interface.

Antigen−Antibody Recognition by Single-Molecule Force Spectroscopy. Force spectroscopy experiments were conducted in order to probe the biological activity of the layers and hence to demonstrate that this technique can be used as a general and dependable method to verify whether the grafted proteins retain their biological recognition capabilities. In order to carry out reliably force spectroscopy measurements, a series of experimental requirements are to be met. First, the binding force of the chemical or biological species onto the tip has to be stronger than

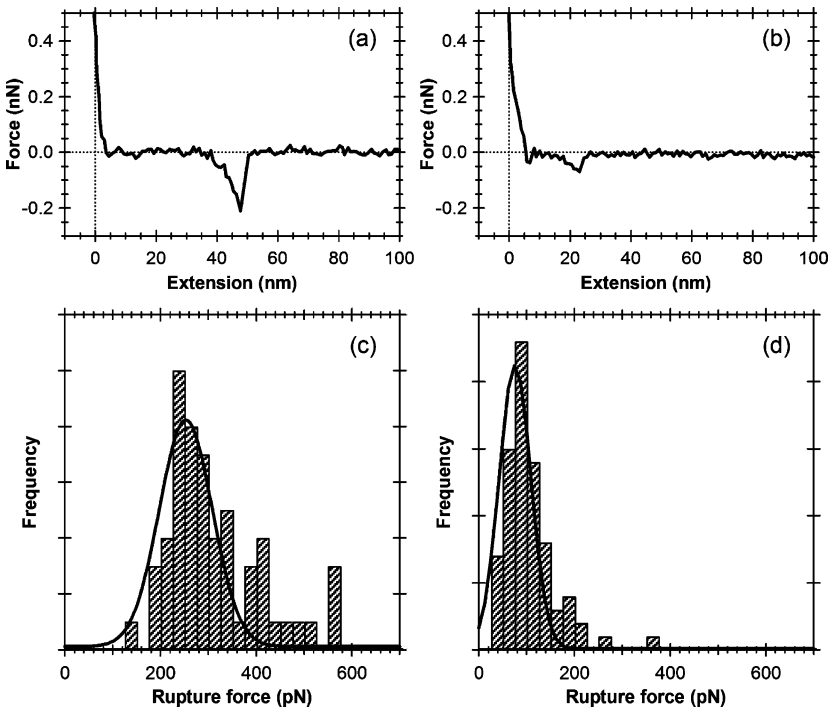

Figure 5. Force−extension curve obtained in a PBS buffer between (a) a 69K Ag-modified surface and a anti-69K Ab-modified tip and (b) a 286F7 Ab-modified surface and a TSH modified tip. Corresponding histograms of the rupture forces: (c) 69K Ag/anti-69K Ab system; (d) 286F7 Ab/TSH system. The curves were recorded at a loading rate of 96 (69K) and 100 nN/s (286F7) (Loading rate-dependent measurements are given in the SI file.).

the investigated interaction strength. Second, the presence of a long-chain spacer linking the species to the tip is required to avoid the interference of nonspecific adhesion forces, which otherwise dominate when tip and surface are close to each other. Here, a *N*-succinimydil acrylate (NSA) polymer was grafted from the tip. As a result, chemisorption ensures strong bonding to the tip,[34] polymerization provides a long-chain spacer, which enables free orientation of the species, while the presence of *N*-succinimydil moieties allows for further functionalization since *N*-succinimydil-activated esters react easily at room temperature with amine functions of whatever protein, giving rise to amide bonds (Scheme 1b). We recently showed that this polymer could be grafted in an isolated chain regime, resulting in the grafting of only one linker at the tip apex, paving the way to its use as a generic platform to probe molecular interactions.[32]

Typical force−distance curves recorded for the two ligand−receptor pairs are shown in Figure 5 (a, c). The curves exhibit sometimes a first weakly negative peak, at short tip-to-surface distance (≤15 nm), which is due to nonspecific adhesion between the tip and the surface. A second negative peak showing up far away from this adhesive force region (>20 nm) reflects the antigen−antibody bond rupture.[35] The value of the force at this latter peak is interpreted as the "unbinding force" of the antigen−antibody complex, which dissociates when the applied pulling force exceeds the bonding strength.[35] The distance at which the bond rupture occurs depends on the position of the protein on the PNSA linker. For a given tip, it should thus always occur at the same distance (see Supporting Information for the characterization of the rupture distance).

The measurement of a large number (more than 250) of force curves, all recorded at the same loading rate of ∼100 nN/s (see Experimental Section), showing an unbinding peak allowed us to construct the force histograms (Figure 5c, d) presenting typical force distributions. The histograms display a close-to-Gaussian profile, whose maximum provides the most probable antigen−antibody rupture force at this loading rate. The force distribution recorded for the 69K Ag/anti-69K Ab couple gives a most probable unbinding force of 256 pN. Likewise, the most probable unbinding force between 286F7 Ab and TSH is 76 pN.

To confirm that the retraction profiles correspond to the stretching of a single linker, the curves were fitted with a wormlike chain model. All the curves could be fitted with the same persistence length (1.1 nm), characteristic of the linker. Details on the mechanical properties of the linker and details on WLC fitting have been published previously.[32,36] In order to probe the homogeneous biological activity of the surfaces, the force curves have been recorded on different points of the sensor surfaces, which demonstrated similar frequencies of unbinding events. For instance, the frequency of unbinding events measured for the 69K Ag sensor surfaces was ∼19% of the force curves recorded, while for 286F7 Ab surfaces was ∼23%. It is worth noting that the frequency of unbinding events for the 69K system measured by SMFS is roughly equal to the frequency of recognition events evaluated from the AFM topographic images, i.e., ∼17%.

In order to confirm that the measured forces do correspond to the rupture of the antigen−antibody complex, the force−

(34) Duwez, A.-S.; Cuenot, S.; Jérôme, C.; Gabriel, S.; Jérôme, R.; Rapino, S.; Zerbetto, F. *Nat. Nanotechnol.* **2006**, *1*, 122.

(35) Schwesinger, F.; Ros, R.; Strunz, T.; Anselmetti, D.; Güntherodt, H. J.; Honegger, A.; Jermutus, L.; Tiefenauer, L.; Plückthun, A. *Proc. Natl. Acad. Sci. U.S.A.* **2000**, *97*, 9972.

(36) Cuenot, S.; Gabriel, S.; Jérôme, R.; Jérôme, C.; Fustin, C.-A.; Jonas, A. M.; Duwez, A.-S. *Macromolecules* **2006**, *39*, 8428.

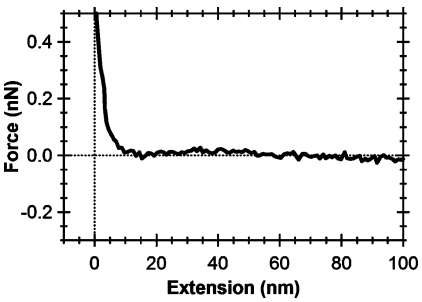

Figure 6. Force−extension curve obtained in a PBS buffer between a 69K Ag-modified surface and a 286F7 Ab-modified tip.

distance curves were compared with those recorded between tip and surface systems not expected to interact with each other. In particular, force−distance curves were recorded between a 69K Ag grafted surface and an unmodified PNSA tip, between a methyl-terminated, self-assembled monolayer surface and a PNSA tip modified with anti-69K Ab, and between a 69K Ag functionalized surface and a PNSA tip modified with 286F7 Ab. A typical force curve recorded between these systems is shown in Figure 6. The retraction curve is characterized by a flat line where only small adhesive forces sometimes appear, testifying for the absence of any specific interaction established between these incompatible pairs.

Based on all these arguments, it can thus be concluded that the rupture peaks observed in Figure 5 were indeed due to the specific interaction between the complementary antigens and antibodies.

CONCLUSIONS

In this paper, we showed that atomic force microscopy measurements performed both in the image mode and in the single-molecule force spectroscopy mode, using a reactive polymer as linker, can be used as a routine technique to rapidly probe the biological activity of biosensor surfaces. AFM images demonstrated that recognition occurred at the sensor surfaces and allowed us to estimate the surface coverage by the sensor proteins, indicating that only a fraction of grafted proteins have reacted with their complementary species. Force measurements probed the biological recognition down to the single ligand−receptor bond, and the force curves recorded between noncomplementary systems validate the specificity of the molecular recognition between complementary species. The main advantage of SMFS is the possibility to carry it out on any substrate, i.e., metallic, semiconducting, or insulating substrates, made of an organic or inorganic material, without restrictions on the size or geometry. The linker used to immobilize the complementary species on the tip is highly versatile and can be used to anchor any (bio)molecule bearing amino-groups.

ACKNOWLEDGMENT

The authors gratefully acknowledge Françoise Blondeau for her technical help, Alexia de Crombrughe for the ellipsometry measurements, Dr. Gaëtane Metz from GlaxoSmithKline Biologicals (Rixensart, Belgium) for providing them with the 69K antigen and the anti-69K antibody, and Dr. Guy Pyrens from BiocodeHycel (Liège, Belgium) for providing the 286F7 antibody. This research was support by the DGTRE of the Wallonia Region (research convention 01/1/5016 “NanoSens”), the Belgian Fund for Fundamental Collective Research (FRFC), and the Belgian Federal Science Policy (IAP network “Supramolecular Chemistry and Supramolecular Catalysis”). F.C. is Postdoctoral Researcher and S.D.-C. and B.N. are Research Associates of the Belgian National Fund for Scientific Research (FNRS).

SUPPORTING INFORMATION AVAILABLE

Additional information as noted in text. This material is available free of charge via the Internet at http://pubs.acs.org.

Received for review January 26, 2007. Accepted June 26, 2007.

AC070155Q